9668 *Macromolecules* **2010**, *43*, 9668–9673
DOI: 10.1021/ma1017617

Macromolecules
ARTICLE

Synthesis and Investigation of Core−Shell Dendritic Nanoparticles with Tunable Thermosensitivity

Guobin Sun and Zhibin Guan*

Department of Chemistry, University of California, 1102 Natural Sciences 2, Irvine, California 92697-2025, United States

Received August 2, 2010; Revised Manuscript Received October 19, 2010

ABSTRACT: A tandem polymerization strategy has been applied to the synthesis of novel core−shell soft nanoparticles having tunable thermosensitivity. These nanoparticles have amphiphilic dendritic core−shell structures, containing dendritic polyethylene (PE) as the hydrophobic core and a layer of poly(oligo((ethylene glycol) methacrylate)s (poly(OEGMA)s) as the hydrophilic shell. The dendritic PE core was first synthesized by chain walking polymerization, which was subsequently grafted with multiple poly(OEGMA) arms by atom transfer radical polymerization (ATRP) of OEGMAs. By varying the composition of the poly(OEGMA) grafts, the thermosensitivity of the core−shell nanoparticles can be tuned with the lower critical solution temperature (LCST) temperature ranging from 20 to 60 °C. Taking advantage of the thermosensitivity and amphiphilicity, the synthesized core−shell nanoparticles show interesting thermosensitive encapsulation of hydrophobic small molecules, which can be utilized for efficient separation of hydrophobic compounds from aqueous solution. This unique type of core−shell nanoparticles may find potential applications in drug formulation and delivery, water treatment, and other nanotechnology applications.

Introduction

Nanoparticles, both inorganic "hard" and organic "soft" nanoparticles, have attracted much attention and been under intensive investigation due to their unique properties and versatile applications as nanomaterials.[1] Among them, stimuli-responsive nanoparticles,[2] possessing interesting chemical and physical properties that can be controlled by different stimuli, have shown a broad range of potential applications including sensors, drug delivery vectors, biomaterials, and separation platforms.[3] With precisely controlled molecular size and architecture, dendrimers are a special type of soft organic nanoparticles.[4,5] Recently, dendrimers with thermo-responsive properties have attracted increasing attention, due to their potential applications in thermally controlled drug delivery and smart matrix-loaded catalysis.[6] Through a core−shell strategy, where a dendrimer acts as the core and a thermosensitive shell is covalently grafted onto the surface of the core to form a dendritic core−shell nanostructure, the dendritic nanoparticles show interesting thermo-responsive properties.[7] As one of the most extensively studied and frequently used thermosensitive polymers,[8] poly(*N*-isopropylacrylamide) (PNIPAAm) has been successfully incorporated to various dendrimers to form thermo-responsive core−shell nanostructures.[9]

Recently, it has been reported that poly(oligo(ethylene glycol) methacrylates) (poly(OEGMAs)) exhibit good thermosensitivity,[10] with comparable and in certain case even superior[11] thermosensitivity compared to PNIPAAm.[8] Like PNIPAAm, the poly(OEGMA) systems have good phase transition reversibility and their lower critical solution temperature (LCST) is relatively independent of external conditions such as pH, concentration.[11] Moreover, with minimal toxicity, poly(OEGMA)s are more biocompatible which will render themselves potential biomedical applications.[12] Recent reports on grafting the poly(OEGMA)s onto inorganic nanoparticles showed these hybrid core−shell nanostructures have interesting thermal-induced properties.[13] However, very scarce work has been done on grafting poly(OEGMA)s onto dendritic organic nanoparticles to form novel core−shell structures.[14]

Our laboratory has developed a convenient one-step procedure, known as chain-walking polymerization (CWP) catalyzed by the Brookhart α-bisimine Pd(II) catalyst,[15] for the copolymerization of ethylene and polar olefin to achieve functional dendritic polyethylene (PE) in one-pot manner.[16] Because these dendritic PEs possess globular structure with highly fractal topology similar to dendrimers, they are more practical alternatives to dendrimers for many potential applications. Introducing thermosensitive properties to our dendritic PEs will result in stimuli-responsive nanostructures, which will further expand the scope of potential applications of our dendritic PE platform. Previously, our laboratory reported a facile synthesis of PE-poly(OEGMA)s (MW of OEGMA 300) dendritic nanoparticles by tandem CWP and ATRP[17] for bioconjugation application.[18] Very recently, Zhang et al. reported an interesting study of temperature-sensitive phase-transition behaviors of the PE-poly(OEGMA) system in aqueous solution using Rayleigh Scattering technique.[19] Herein, we report the synthesis and investigation of dendritic PE−poly(OEGMA) core−shell nanoparticles with tunable thermosensitivity (Scheme 1).

Specifically, the tunability of thermal sensitivity was achieved by varying the composition of the hydrophilic shell layer which was conveniently controlled by the ratio of two different OEGMA monomers: **A** ($n = 2$, 2-(2′-methoxyethoxy)ethyl methacrylate) and **B** ($n = 8.4$, average M_n 475). The homopolymers of individual **A** and **B** have LCST's at 26 and 90 °C, respectively.[10a,c] By adjusting the ratio of **A** and **B** in the copolymers, thermosensitivity of the shell is tunable so that the core−shell nanostructures can show controllable thermosensitivity with various LCST. In light of their thermosensitivity and amphiphilicity, we have further investigated the capability of the core−shell nanoparticles for encapsulation of hydrophobic molecules such as Nile

*Corresponding author. E-mail: zguan@uci.edu.

 Published on Web 11/10/2010

Scheme 1. Synthesis of Dendritic Core−Shell Nanoparticles with Tunable Thermosensitivity by ATRP of Poly(OEGMA)s on Dendritic PE Core

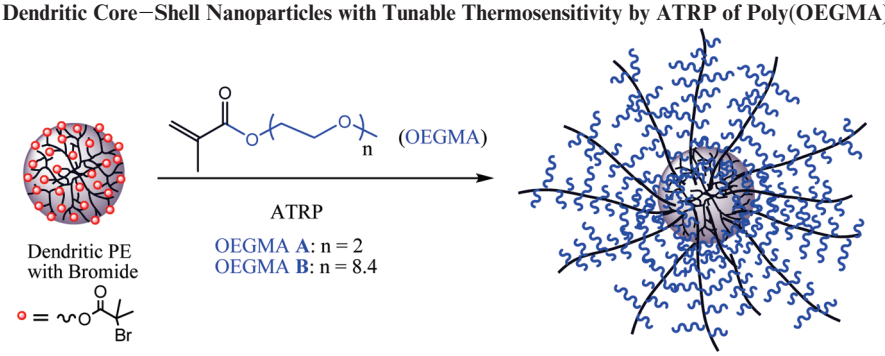

Table 1. Synthesis and Characterization of Dendritic Core−Shell Nanoparticles by ATRP[a]

polymer sample	[A]/[B][b] (in feed)	M_n (10^6 D)[c]	PDI[c]	[A]/[B][d] (in polymer)	LCST (°C)[e]	D_h(THF) (nm)[f]	D_h(H_2O) (nm)[g]
1	100/0	2.64	1.35	100/0	18.6	28.9	N/A
2	96.5/3.5	5.40	1.24	96.3/3.7	29.3	32.7	25.3
3	92.0/8.0	3.85	1.17	94.0/6.0	34.1	37.9	21.5
4	85.0/15.0	4.23	1.08	88.0/12.0	42.6	32.1	23.3
5	77.5/22.5	4.77	1.32	81.9/18.1	49.5	33.0	28.4
6	70.0/30.0	5.22	1.26	73.0/27.0	58.9	37.0	27.3

[a] [Br]: [CuBr]: [$CuBr_2$]: [dNbPy]: [OEGMA] = 1: 2: 0.2: 4.8: 80.0 (dNbPy: 4,4′-dinonyl-2,2′-dipyridyl), in anisole at room temperature. [b] Feeding molar ratio. [c] By SEC-coupled MALLS detector in THF (1 mL/min). [d] Molar ratio in polymers calculated from ^{1}H NMR. [e] Measured with a concentration of 5.0 mg/mL in aqueous solution, temperature increase at 1 °C/min. [f] Measured by DLS with 1.0 mg/mL concentration in THF at 25 °C. [g] Measured by DLS with 1.0 mg/mL concentration in water at 25 °C. Both D_h values are by number-average.

Red (NR) and the temperature dependent properties of the dye-encapsulated nanoparticles.

Results and Discussion

Synthesis of the Core−Shell Nanostructures. The synthesis was achieved by the tandem CWP-ATRP approach as described previously (Scheme 1).[18] Briefly, a dendritic PE core containing multiple ATRP initiation sites was first synthesized by chain-walking copolymerization of ethylene (0.1 atm) and a bromine-containing olefin (2-bromo-2-methyl-propionic acid-1,1-dimethyl-but-3-enyl ester) using the Brookhart Pd(II)-α-bisimine catalyst. On the basis of ^{1}H NMR and M_n data, each PE contains ~470 ATRP initiation sites (see Experimental Section).OEGMA **A** and OEGMA **B** with different mole ratio were successfully (co)polymerized onto the PE core via ATRP to form the desired core−shell nanostructures **1**−**6** (Table 1).

Characterization of the Dendritic Core−Shell Nanoparticles. The molecular weights of these core−shell nanoparticles were determined by SEC coupled with a multiangle laser light scattering (MALLS) detector. All of these polymers **1**−**6** show high molecular weight and relatively narrow polydispersity (Table 1). The ratio of **A** and **B** in the polymers after ATRP was calculated from ^{1}H NMR, which is close to the feeding ratio for the copolymerization, indicating that the copolymerization reactivity of **A** and **B** is similar. Particle size of these polymers was also measured by dynamic light scattering (DLS). As expected, the particle size in THF solution is larger than that in aqueous solution for each polymer, because the PE core is fully solvated in THF but collapses in water, thus decreasing the overall size of the entire nanoparticles.

Thermosensitivities of the polymers **1**−**6** were measured in aqueous solutions by monitoring the transmittance at 650 nm for each polymer solution, and sharp phase changes near LCST for each polymer were observed for all samples, showing that they have good thermal-responsive abilities (Figure 1). By tuning the composition of the hydrophilic shell of our core−shell nanoparticles, their thermosensitivity, and

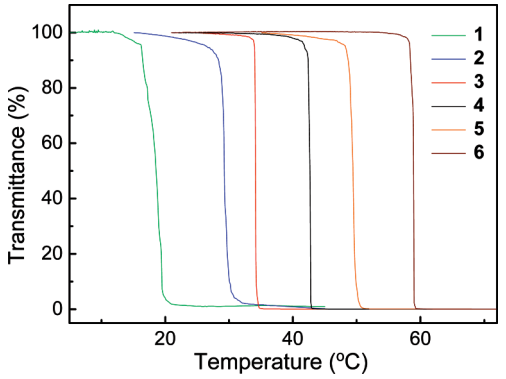

Figure 1. LCST measurement by transmittance versus temperature curves (λ = 650 nm, 1 °C/min). From left to right, the six graphs stands for polymer **1**−**6** (polymer concentration: 5 mg/mL).

thus LCST, is tunable. The measured LCST values have a direct dependence on molar ratio of **B** in these polymers: the higher ratio of **B**, the higher LCST value. This trend is reasonable, because hydrophobicity to hydrophilicity ratio in thermosensitive polymers affects their LCST values, and hydrophobicity decreases the LCST while hydrophilicity increases it.[20] Although backbone of the poly(**A**-*co*-**B**)s is hydrophobic, their side chain oligo(ethylene glycol) (OEG) is hydrophilic. **B** has a longer OEG side chain so is more hydrophilic than **A**,[21] thus increasing ratio of **B** increases hydrophilicity of the whole polymer structure. From **1** to **6**, these polymers have a universal decreasing hydrophobicity and increasing hydrophilicity, so their LCST value increases, correspondingly.

It was reported that linear poly(**A**-*co*-**B**) copolymers showed good thermal-responsive abilities. By varying the molar ratio of **A** and **B**, their thermosensitivity is tunable,[10d] and the measured LCST values have a good linear dependence on molar ratio of **B** in these linear copolymers (Figure 2, square). Compared with these linear poly(**A**-*co*-**B**)s, LCST values of polymers **1**−**6** have slightly different dependences on the molar ratio of **B**. When the molar ratio of

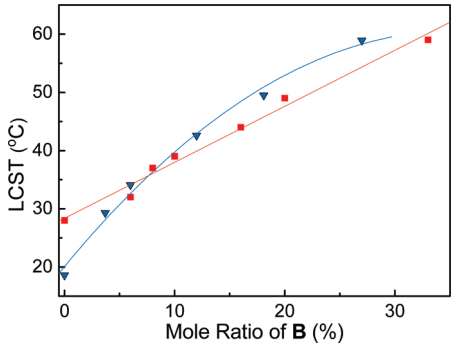

Figure 2. Relationship between the measured LCST values and the composition molar ratio of **B** in polymers (square, linear poly(**A**-*co*-**B**)s;[10d] triangle, core−shell dendritic polymers **1**−**6**).

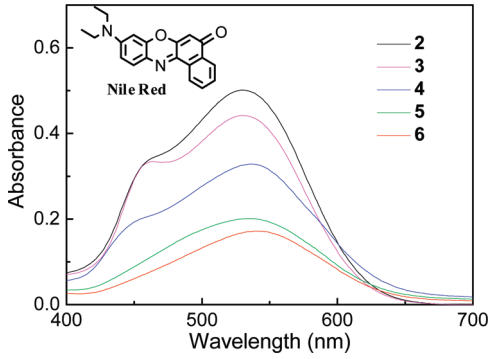

Figure 3. UV−vis spectra of NR encapsulated by polymers **2**-**6** in aqueous solutions (polymer concentration: 1 mg/mL).

B is relatively low (0−5%), the LCST values of the dendritic core−shell polymers are lower than those of the linear poly(**A**-*co*-**B**)s at the same **A**/**B** ratio; while when the molar ratio of **B** is above 10%, the trend is reversed and the LCST is slightly higher than those of the linear poly(**A**-*co*-**B**)s.

We think two effects in the core−shell structures might contribute to the difference in LCST dependence on polymer composition. First of all, the PE core is hydrophobic which increases the hydrophobicity of the whole polymer structure thus decreasing its LCST.[20] This effect is more pronounced when the whole polymer contains less amount of the more hydrophilic **B** (molar ratio $< 5\%$). At higher molar ratio of the more hydrophilic **B**, the influence of the hydrophobic PE core is diminishing. Second, all the linear polymers are tethered onto the core, and this tethering effect helps to increase the LCST. The reason is that when the temperature is below LCST, these poly(**A**-*co*-**B**)s (tethered or untethered) are soluble in water, because a layer of water molecules are surrounding their OEG side chains to ensure the water solubility.[21] When the temperature is above LCST, these bound water molecules are released into bulky solvent then these poly(**A**-*co*-**B**)s become insoluble and tend to aggregate.[8,21] This is because in the dendritic core−shell polymer, the tethered poly(**A**-*co*-**B**)s congest in the limited shell space so the amount of bound water molecules is less than that of the untethered linear poly(**A**-*co*-**B**)s. Thus, the entropy gain due to water molecule release during this phase change for the tethered polymers is smaller than that for the corresponding linear free polymers, which then requires higher temperature for compensation. Nevertheless, the LCST of the tethered poly(**A**-*co*-**B**)s is only slightly higher than that of the corresponding linear poly(**A**-*co*-**B**)s. Therefore, the difference in entropy gains during the phase change is relatively small. Overall, when the molar ratio of **B** is above 10%, the LCST of the dendritic polymers can be considered to be very close to those of the corresponding free poly(**A**-*co*-**B**)s.

Encapsulation Studies of Nile Red (NR) in Aqueous Solution. To investigate the delivering capabilities of these polymers **1**-**6** in water, NR, an excellent UV−vis probe,[22] was selected as the model molecule of hydrophobic drugs for encapsulation study. Because the LCST of polymer **1** is lower than room temperature, it was not included in the encapsulation study. NR was successfully encapsulated by polymers **2**−**6** in aqueous solution. The clear polymer solution with pink color which comes from encapsulated NR was then analyzed by means of UV−vis spectroscopy (Figure 3). Polymers **2**−**6** showed different encapsulation abilities; based on the UV−vis absorbance (after background subtraction) at λ_{max}, calculation shows that the amount of NR encapsulated by same mole amount of polymers from **2**−**6** has a ratio of 1.00:0.62:0.51:0.35:0.33, with a trend that the higher molar ratio of **A** in these polymers, the more NR they can encapsulate. Since all of these polymers have the same hydrophobic PE core, the polymers should have similar ability to encapsulate NR if only the core encapsulates the NR. On the basis of this observation, we propose that not only the core, but also the tethered poly(**A**-*co*-**B**)s in the shell engage in the encapsulation. This assumption is reasonable, because in the congested shell space, density of these poly(**A**-*co*-**B**)s are so high that their hydrophobic backbones aggregate to form some hydrophobic domains,[23] which, together with the hydrophobic core, help to encapsulate more NR molecules.

This proposal is supported by previous literature reports which observed aggregation behavior of poly(OEGMA)s in aqueous solution:[23] once the poly(OEGMA)s was above certain concentration (critical aggregation concentration CAC), they aggregated into micelles by forming hydrophobic domain from the polymethacrylate backbone and hydrophilic domain from the short OEG chains.[23] This is further supported by the blue shift in λ_{max} of encapsulated NR for core−shell polymers **6** to **2** having more hydrophobic shell composition. From polymers **6** to **2**, with increasing ratio of more hydrophobic OEGMA **A**, the λ_{max} shifts from 542 to 530 nm (Figure 3), indicating increasingly more hydrophobic environment for the encapsulated NR within these polymers.[24] Previously our laboratory reported the synthesis of water-soluble dendritic polymers containing dendritic hydrophobic PE core and a layer of linear hydrophilic poly(ethylene glycol)s (PEG, M_n ~800) as the shell, and their application as molecular nanocarriers in aqueous solution.[16b] Encapsulated NR by these molecular nanocarriers shows λ_{max} at ~550 nm. Compared with the molecular nanocarriers, polymers **2**−**6** contain poly(OEGMA)s in the shell, which are more hydrophobic than the PEG, in turn rendering them a more hydrophobic environment for NR encapsulation. This explains why NR encapsulated by polymers **2**−**6** all has blue shift in λ_{max} (530−542 nm) compared to NR encapsulated by the PE−PEG nanocarriers[16b] (λ_{max} 550 nm). Furthermore, from polymers **6** to **2**, with increasing ratio of more hydrophobic **A**, there is a growing shoulder (Figure 3) below 500 nm, indicating a more hydrophobic microenvironment[24] encapsulating some of the NR in aqueous solution, as an additional evidence that some of these encapsulated NR stays in the more hydrophobic domains[24] resulting from assembly of these tethered poly(**A**-*co*-**B**)s. These more hydrophobic domains might be directly from self-assembly of the polymethacrylate backbones, or from part of the PE core next to the self-assembled polymethacrylate backbones. A similar phenomenon has also been observed by Haag and cowrokers for NR encapsulation due to changing environment of increasing nonpolarity.[24]

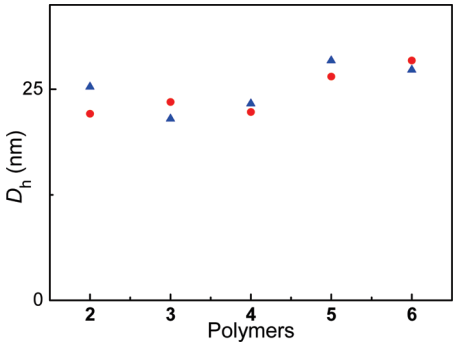

Figure 4. DLS measurement of nanoparticle sizes in the aqueous solutions of polymers **2**−**6** with (triangle) or without (circle) encapsulated NR (polymer concentration: 1 mg/mL).

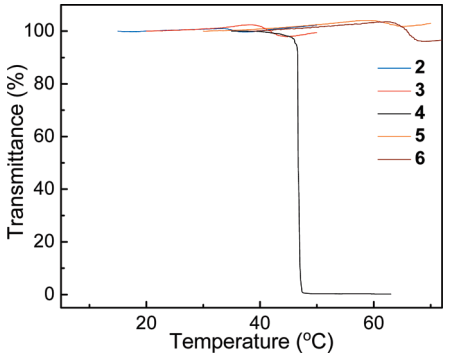

Figure 5. LCST measurement for NR-encapsulated polymers **2**-**6** by transmittance versus temperature curves (polymer concentration 5.0 mg/mL, $\lambda = 650$ nm, 1 °C/min).

In some previous studies, encapsulation of hydrophobic compounds by core−shell nanostructures induced aggregation of the nanoparticles.[25] To confirm the encapsulation of NR by our core−shell polymers was through unimolecular mechanism, the sizes of the nanoparticle were measured by DLS before and after NR encapsulation. It showed that the nanoparticle size (D_h, hydrodynamic diameter) did not have any obvious change before and after encapsulation (Figure 4). This excludes the possibility of interparticle aggregation after NR encapsulation and provides strong evidence for the unimolecular encapsulation behavior of the amphiphilic core−shell nanoparticles in aqueous solution. This also confirms that the different encapsulation capacities of polymers **2**−**6** are due to their own molecular structures, instead of other secondary effects such as interpolymer interactions.[25]

Thermosensitivity of these polymers after NR encapsulation was also studied which, to our surprise, turned out to be quite different from the corresponding polymers before encapsulation (Figure 5). Polymer **4** with NR encapsulated showed sharp phase change near its LCST of 46.6 °C, which is slightly different from the LCST of the blank polymer **4** solution (42.6 °C). However, the NR-encapsulated polymer **2**, **3**, **5**, and **6** solutions kept transparent upon heating for short time and did not showed obvious phase change. After the hot turbid solution of NR-encapsulated polymer **4** was filtered through a 0.2 μm syringe filter and then cooled to room temperature, the NR UV−vis absorbance dropped by 91.2%, indicating that 91.2% of the encapsulated NR was retained in the precipitated polymer. For the aqueous solution of NR-encapsulated polymer **3**, although it did not show obvious phase transition upon heating for short time, a clear phase change was observed after heating at 75 °C overnight. The turbid solution of polymer **3** was also filtered when hot and the NR UV−vis absorbance dropped by 96.8% of the original value, indicating that 96.8% of the encapsulated NR was retained in the precipitated polymer. On the contrary, the solutions of NR-encapsulated polymer **2**, **5**, and **6** remained transparent even after being heated at 75 °C overnight. Following the same procedure of filtration while hot, the NR UV−vis absorbance of polymers **2**, **5**, and **6** dropped by only 20.5%, 4.7%, and 16.2%, respectively. However, when the feeding ratio of NR for encapsulation was decreased by 3 times, the solution of polymer **2**, **5**, and **6** became turbid after being heated at 75 °C overnight. These turbid solutions were filtered when hot and their NR UV−vis absorbance all dropped by >99%, indicating that most of the encapsulated NR was retained in the precipitated polymers. In summary, the excellent thermally induced separation of NR in aqueous solution achieved by these polymers, especially polymer **4,** is noteworthy,[26] showing their potentials for applications including thermally triggered separations, water treatment, and drug delivery. The encapsulation of NR by polymer **2**, **3**, **5**, and **6** has a more complicated influence on their thermosensitivity. Apparently not only the hydrophobicicity/hydrophilicity ratio of the polymer structure, but also interaction between the core−shell nanostructures and the encapsulated NR guest molecules change their thermosensitivity. Similar complicated influence of encapsulated guest molecules on thermosensitivity was observed for other dendrimer systems, which also suggests interaction between the guest molecules and the dendrimer nanostructures may play an important role on controlling their thermosensitivity.[26b]

Conclusion

In summary, we have successfully prepared a series of amphiphilic core−shell polymers having hydrophobic dendritic PE core and thermosensitive poly(OEGMA) shell. The polymers were synthesized by a facile tandem CWP-ATRP strategy. By varying the composition of the poly(OEGMA) shell, the thermosensitivity of the core−shell dendritic nanoparticles can be controlled with the LCST ranging from 18 to 60 °C. The synthesized core−shell nanoparticles showed good encapsulation capacity for hydrophobic molecules such as NR. The UV−vis spectra and DLS studies on NR encapsulation in aqueous solutions confirmed unimolecular behavior of these systems. Furthermore, polymers **3** and **4** show excellent thermally triggered separation ability for the encapsulated hydrophobic guest molecules. Combined with their good aqueous solubility and biocompatibility of the OEG system,[12,13] the reported core−shell nanoparticles may find various potential applications such as thermo-controllable drug delivery and release, separation platform, and water treatment.

Experimental Section

Materials. All chemicals were purchased from Sigma-Aldrich. 2-(2′-Methoxyethoxy)ethyl methacrylate (**A**) and poly(ethylene glycol) methyl ether methacrylate (**B**, M_n 475) were passed through active neutral alumina gel prior to use. Copper(I) bromide (CuBr 99.999%), copper(II) bromide ($CuBr_2$ 99+%) and 4,4′-dinonyl-2,2′-dipyridyl (dNbpy, 97%) were used as received. Anisole was distilled and bubbled by Argon prior to use. Tetrahydrofuran (THF) and methanol were used as received. Spectra/Por Dialysis Membrane (MWCO 50, 000) was purchased from Fisher and rinsed and soaked in DI-water for 1 h before use.

Instrumentation. NMR spectra were measured on Bruker GN500 and Bruker Cryo500 MHz FT-NMR instruments. ^{1}H NMR spectra were recorded in ppm and referenced to the indicated deuterium solvent ($CDCl_3$). UV/vis spectra were recorded on a JASCO V-530 UV/vis dual-beam spectrophotometer,

which used deuterium lamp as light source for UV range (190−350 nm) and halogen lamp for Vis range (330−1100 nm). The particle sizes in THF solution by dynamic light scattering (DLS) were measured on a Zetasizer Nano Series (Malvern Instrument, Model: ZEN3600) at 25 °C. All other moisture and air-sensitive reactions were carried out in flame-dried glassware charged with a positive pressure of argon. All of the reported polymers were characterized by size-exclusion chromatography (SEC) in THF (1.0 mL/min) coupled with a multiangle laser light scattering (MALLS) detector and refractometric index (RI) detector. Measurement were made on highly dilute fractions eluting from a SEC consisting of a HP Agilent 1100 solvent delivery system/auto injector with an online solvent degasser, temperature-controlled column compartment. A Dawn DSP 18-angle laser light scattering detector (MALLS, laser wavelength λ = 632 nm, Wyatt Technology, Santa Babara, CA) was coupled to the SEC. A 30 cm column was used (Polymer Laboratories PLgel Mixed C, 5 μm particle size) to separate polymer samples at 35 °C. A 60 μL of a 2 mg/mL solution was injected into the column. Software ASTRA 4.7 from Wyatt Technology was used to acquire data from the MALLS. The M_w and M_n data were obtained by following classical light scattering treatments. Removal of all the organic solvents was accomplished by rotary evaporation and is referred to as concentrated *in vacuo*.

Synthesis of Bromine-Containing Dendritic PE Core. The PE core was synthesized by following our reported procedure.[18] In brief, 2-bromo-2-methyl-propionic acid-1,1-dimethyl-but-3-enyl ester (1.88 g, 7.14 mmol) and Brookhart Pd(II)−bisimine catalyst (38 mg, 0.025 mmol) were dissolved in chlorobenzene (4.0 mL) and toluene (4.0 mL). Under stirring, the above solution was bubbled with ethylene (0.1 atm) for 2 days at room temperature. After quenched by excess amount of Et_3SiH, to the solution was added 100 mL of toluene. Then it was passed through Celite to remove residue pallidum(0). The solvent was removed *in vacuo* and the residue was redissolved in small amount of THF. Then it was precipitated in large excess of methanol. The dissolution/precipitation process in THF/methanol was repeated two more times. It was dried under high vacuum to yield the bromide-containing PE 2.23 g. SEC based on PS−styrene calibration: M_n = 51 300 g/mol, M_w = 92 800 g/mL, DPI = 1.81. SEC−MALLS: M_n = 218 400 g/mol, M_W = 409,700 g/mL, DPI = 1.88. ^{1}H NMR (500 MHz, $CDCl_3$), δ: 3.87 (s, 2H), 1.94 (s, 6H), 1.4−1.0 (br, 31.1H), 1.0−0.8 (br, 9.8H). On the basis of ^{1}H NMR and M_n (SEC−MALLS) data, each PE contains ~470 bromide atoms.

General ATRP Procedure for the Synthesis of Polymer 1−6.[18,27] [Initiator]/[CuBr] /[$CuBr_2$]/[dNbPy] /[OEGMA] molar ratio ([Initiator] refers to [−C(O)C(Me)$_2$Br] on the dendritic PE; [OEGMA] refers to total concentration of monomer **A** and **B**) at 1/2/0.2/4.8/80 was used for all of the ATRP reactions. In a typical experiment the dendritic PE (0.040 g, 0.10 mmol initiator) was dissolved in degassed anisole (12 mL) with OEGMA **A** (1.48 mL, 8.00 mmol) and dNbpy (0.198 g, 0.48 mmol) and purged with dry argon for 15 min. CuBr (29.0 mg, 0.20 mmol) and $CuBr_2$ (4.5 mg, 0.02 mmol) were quickly added into a flask and subjected for three cycles of evacuate/purge under argon and then added into the above solution. The mixture was subjected 3 cycles of freeze/pump/thaw to remove any residue oxygen. After charged with argon the reaction was stirred at room temperature for 12 h. Then the reaction was quenched by exposed to air and diluted with methanol before dialysis against methanol for purification to yield polymer **1** (357 mg). ^{1}H NMR (500 MHz, $CDCl_3$), δ: 4.12 (s, 2H), 3.82−3.48 (br, 7.12H), 3.46−3.35 (br, 3.61H), 2.20−1.75 (br, 1.56H), 1.38−0.70 (br, 6.53H).

*Polymer **2***. OEGMA **A** (1.43 mL, 7.72 mmol) and OEGMA **B** (0.12 mL, 0.28 mmol) were used following the similar procedure described above. Yield: 550 mg. ^{1}H NMR (500 MHz, $CDCl_3$), δ: 4.11 (s, 2H), 3.82−3.48 (br, 8.64H), 3.46−3.35 (br, 3.90), 2.20−1.75 (br, 1.48H), 1.38−0.70 (br, 4.86H).

*Polymer **3***. OEGMA **A** (1.36 mL, 7.36 mmol) and OEGMA **B** (0.27 mL, 0.64 mmol) were used following the similar procedure described above. Yield: 448 mg. ^{1}H NMR (500 MHz, $CDCl_3$), δ: 4.12 (s, 2H), 3.82−3.48 (br, 9.80H), 3.46−3.35 (br, 3.88H), 2.20−1.75 (br, 1.37H), 1.38−0.70 (br, 5.60H).

*Polymer **4***. OEGMA **A** (1.25 mL, 6.80 mmol) and OEGMA **B** (0.50 mL, 1.20 mmol) were used following the similar procedure described above. Yield: 336 mg. ^{1}H NMR (500 MHz, $CDCl_3$), δ: 4.12 (s, 2H), 3.82−3.48 (br, 11.56H), 3.46−3.35 (br, 3.82), 2.20−1.75 (br, 1.30H), 1.38−0.70 (br, 4.90H).

*Polymer **5***. OEGMA **A** (1.15 mL, 6.20 mmol) and OEGMA **B** (0.75 mL, 1.80 mmol) were used following the similar procedure described above. Yield: 547 mg. ^{1}H NMR (500 MHz, $CDCl_3$), δ: 4.11 (s, 2H), 3.82−3.48 (br, 13.46H), 3.46−3.35 (br, 3.82), 2.20−1.75 (br, 1.42H), 1.38−0.70 (br, 5.32H).

*Polymer **6***. OEGMA **A** (1.03 mL, 5.60 mmol) and OEGMA **B** (1.00 mL, 2.40 mmol) were used following the similar procedure described above. Yield: 570 mg. ^{1}H NMR (500 MHz, $CDCl_3$), δ: 4.12 (s, 2H), 3.82−3.48 (br, 19.07H), 3.46−3.35 (br, 4.42H), 2.20−1.75 (br, 1.14H), 1.38−0.70 (br, 6.39H).

General Procedure for NR Encapsulation. Uptake of NR was successfully accomplished at room temperature following a few consecutive steps. First of all, the polymer and NR (1% of the polymer by weight) were homogeneously mixed by dissolving in organic solvent, and after that the solvent was removed under vacuum; to the residue was added certain amount of water and the above mixture was stirred overnight. Then the mixture stood for a few hours and was filtered via 0.2 μm cellulose ester syringe filter to remove any trace amount of unsolubilized NR. The clear polymer solution was then analyzed by UV−vis spectroscopy. The absorbance of encapsulated NR (after background subtraction) at λ_{max} for the polymers from **2−6** has a ratio of 1:0.88:0.65:0.40:0.34.

Acknowledgment. We are very thankful to the National Science Foundation (CHE-0456719, CHE-0723479 and DMR-0703988) for the financial support. We also thank Dr. Phil Dennison and Dr. Wytze van der Veer for valuable assistance with NMR, DLS and UV-vis measurements. Z.G. acknowledges a Camille Dreyfus Teacher−Scholar Award.

References and Notes

(1) (a) De, M.; Ghosh, P. S.; Rotello, V. M. *Adv. Mater.* **2008**, *20*, 4225–4241. (b) Taton, D.; Feng, X.; Gnanou, Y. *New J. Chem.* **2007**, *31*, 1097–1110. (c) Gao, H.; Yang, Y.-W.; Fan, Y. G.; Ma, J. B. *J. Controlled Release* **2006**, *112*, 301–311. (d) Moghimi, S. M.; Hunter, A. C.; Murray, J. C. *FASEB J.* **2005**, *19*, 311–330. (e) Smith, D. K.; Hirst, A. R.; Love, C. S.; Hardy, J. G.; Brignell, S. V.; Huang, B. *Prog. Polym. Sci.* **2005**, *30*, 220–293. (f) Tomalia, D. A. *Prog. Polym. Sci.* **2005**, *30*, 294–324.

(2) (a) Ballauff, M.; Lu, Y. *Polymer* **2007**, *48*, 1815–1823. (b) Arshady, R. *MML Series* **2006**, *7*, 11–41.

(3) (a) Ganta, S.; Devalapally, H.; Shahiwala, A.; Amiji, M. *J. Controlled Release* **2008**, *126*, 187–204. (b) Fabris, L.; Dante, M.; Nguyen, T. Q.; Tok, J. B. H.; Bazan, G. C. *Adv. Funct. Mater.* **2008**, *18*, 2518–2525.

(4) (a) Tomalia, D. A.; Baker, H. D.; Dewald, J.; Hall, J. M.; Kallos, G.; Martin, R.; Ryder, J. *Polym. J.* **1985**, *17*, 117–132. (b) Newkome, G. R.; Yao, Z.; Baker, G. R.; Gupta, V. K. *J. Org. Chem.* **1985**, *50*, 2003–2004.

(5) Hawker, C. J.; Fréchet, J. M. J. *J. Am. Chem. Soc.* **1990**, *112*, 7638–7647.

(6) (a) Haag, R.; Pickaert, G. *MML Ser.* **2006**, *7*, 153–210. (b) Li, W.; Zhang, A.; Chen, Y.; Feldman, K.; Wu, H.; Schlüter, A. D. *Chem. Commun.* **2008**, 5948–5950.

(7) Kojima, C.; Tsumura, S.; Harada, A.; Kono, K. *J. Am. Chem. Soc.* **2009**, *131*, 6052–6053.

(8) Dimitrov, I.; Trzebicka, B.; Müller, A. H. E.; Dworak, A.; Tsvetanov, C. B. *Prog. Polym. Sci.* **2007**, *32*, 1275–1343.

(9) (a) You, Y. Z.; Hong, C. Y.; Pan, C. Y.; Wang, P. H. *Adv. Mater.* **2004**, *16*, 1953–1957. (b) Xu, H.; Xu, J.; Zhu, Z.; Liu, H.; Liu, S. *Macromolecules* **2006**, *39*, 8451–8455. (c) Xu, J.; Luo, S.; Shi, W.; Liu, S. *Langmuir* **2006**, *22*, 989–997.

(10) (a) Han, S.; Hagiwara, M.; Ishizone, T. *Macromolecules* **2003**, *36*, 8312–8319. (b) Kitano, H.; Hirabayashi, T.; Gemmei-Ide, M.; Kyogoku M. *Macromol. Chem. Phys.* **2004**, *205*, 1651–1659. (c) Mertoglu, M.; Garnier, S.; Laschewsky, A.; Skrabania, K.; Storsberg, J. *Polymer* **2005**, *46*, 7726–7740. (d) Lutz, J. -F.; Hoth, A. *Macromolecules* **2006**, *39*, 893–896. (e) Becer, C. R.; Hahn, S.; Fijten, M. W. M.; Thijs, H. M. L.; Hoogenboom, R.; Schubert, U. S. *J. Polym. Sci., Part A: Polym. Chem.* **2008**, *46*, 7138–7147.
(11) Lutz, J. -F.; Akdemir, Ö.; Hoth, A. *J. Am. Chem. Soc.* **2006**, *128*, 13046–13047.
(12) Lutz, J. -F. *J. Polym. Sci., Part A: Polym. Chem.* **2008**, *46*, 3459–3470.
(13) (a) Lutz, J. -F.; Stiller, S.; Hoth, A.; Kaufner, L.; Pison, U.; Cartier, R. *Biomacromolecules* **2006**, *7*, 3132–3138. (b) Li, D.; Jones, G. L.; Dunlap, J. R.; Hua, F.; Zhao, B. *Langmuir* **2006**, *22*, 3344–3351. (c) Edwards, E. W.; Chanana, M.; Wang, D.; Möhwald, H. *Angew. Chem., Int. Ed.* **2008**, *47*, 320–323. (d) Hucknall, A.; Rangarajan, S.; Chilkoti, A. *Adv. Mater.* **2009**, *21*, 2441–2446.
(14) Saha, A.; Ramakrishnan, S. *Macromolecules* **2008**, *41*, 5658–5664.
(15) Ittel, S. D.; Johnson, L. K.; Brookhart, M. *Chem. Rev.* **2000**, *100*, 1169–1203.
(16) (a) Chen, G.; Ma, X. S.; Guan, Z. *J. Am. Chem. Soc.* **2003**, *125*, 6697–6704. (b) Chen, G.; Guan, Z. *J. Am. Chem. Soc.* **2004**, *126*, 2662–2663.
(17) Matyjaszewski, K.; Xia, J. *Chem. Rev.* **2001**, *101*, 2921–2990.
(18) Chen, G.; Huynh, D.; Felgner, P. L.; Guan, Z. *J. Am. Chem. Soc.* **2006**, *128*, 4298–4302.
(19) Zhang, L.; Su, J.; Zhang, W.; Ding., M.; Chen, X.; Wu, Q. *Langmuir* **2010**, *26*, 5801–5807.
(20) (a) Zou, Y.; Brooks, D. E.; Kizhakkedathu, J. N. *Macromolecules* **2008**, *41*, 5393–5405. (b) Tono, Y.; Kojima, C.; Haba, Y.; Takahashi, T.; Harada, A.; Yagi, S.; Kono, K. *Langmuir* **2006**, *22*, 4920–4922.
(21) (a) Karlström, G.; Carlsson, A.; Lindman, B. *J. Phys. Chem.* **1990**, *94*, 5005–5015. (b) Ganji, F.; Abdekhodaie, M. J. *Carbohydr. Polym.* **2008**, *74*, 435–441.
(22) Watkins, D. M.; Sayed-Sweet, Y.; Klimash, J. W.; Turro, N. J.; Tomalia, D. A. *Langmuir* **1997**, *13*, 3136–3141.
(23) Hussain, H.; Mya, K. Y.; He, C. *Langmuir* **2008**, *24*, 13279–13286.
(24) Burakowska, E.; Haag, R. *Macromolecules* **2009**, *42*, 5545–5550.
(25) Radowski, M. R.; Shukla, A.; von Berlepsch, H.; Böttcher, C.; Pickaert, G.; Rehage, H.; Haag, R. *Angew. Chem., Int. Ed.* **2007**, *46*, 1265–1269.
(26) (a) Aathimanikandan, S. V.; Savariar, E. N.; Thayumanavan, S. *J. Am. Chem. Soc.* **2005**, *127*, 14922–14929. (b) Kono, K.; Miyoshi, T.; Haba, Y.; Murakami, E.; Kojima, C.; Harada, A. *J. Am. Chem. Soc.* **2007**, *129*, 7222–7223.
(27) Jakubowski, W.; Matyjaszewski, K. *Macromolecules* **2005**, *38*, 4139–4146.